PHYSICAL REVIEW B VOLUME 49, NUMBER 3 15 JANUARY 1994-I

Adsorption, thermal reaction, and desorption of disilane on Ge(111)-$c(2\times8)$

D.-S. Lin, E. S. Hirschorn, T. Miller, and T.-C. Chiang

Department of Physics, University of Illinois, 1110 West Green Street, Urbana, Illinois 61801-3080
and Materials Research Laboratory, University of Illinois, 104 South Goodwin Avenue, Urbana, Illinois 61801-2902

(Received 23 August 1993)

Room-temperature adsorption of disilane (Si_2H_6) on Ge(111)-$c(2\times8)$ and subsequent thermal reactions and desorption at elevated temperatures were studied using scanning tunneling microscopy and core-level photoemission. The initial adsorption results in the formation of various surface radicals, and the reacted areas on the surface grow laterally for increasing exposures. The sticking coefficient is rather low, and an exposure greater than about 30 000 langmuirs is needed to saturate the surface. The net amount of Si deposited for the saturated surface is about one-half of an atomic layer. Thermal annealing causes the hydrogen atoms to desorb and the Si atoms to move below the surface. For annealing temperatures beyond about 630 K, the desorption of hydrogen becomes complete, all of the Si atoms move below the surface, and the resulting surface resembles the starting clean Ge(111)-$c(2\times8)$ surface except that the $c(2\times8)$ long-range order is partially destroyed. Step flow and island coarsening, similar to growth by molecular-beam epitaxy, are observed.

I. INTRODUCTION

Vapor-phase epitaxy has long been the standard technique for thin-film deposition in silicon integrated circuit manufacturing.[1] The surface chemical reactions and growth mechanisms involved in this process have attracted much technological and scientific interest. Numerous efforts have been made on the optimization of the growth processes and characterization of the resulting film properties. To this end, a variety of experimental techniques have been employed, including electron and optical spectroscopy, electron and x-ray diffraction, electron microscopy, scanning tunneling microscopy (STM), etc. Of all of these techniques, only STM provides a direct view, with atomic resolution, of the surface structure. However, STM by itself does not permit an easy identification of atomic species. Thus, to gain a detailed understanding of crystal growth where more than one atomic species is present, it is important to combine the power of STM with other techniques that are sensitive to the atomic composition near the surface. Core-level photoemission spectroscopy, with its high surface and site sensitivity, is particularly suitable for this task.[2,3] It allows the differentiation of different kinds of atoms, atoms in different chemical-bonding environments (chemical shifts), and atoms on the surface as opposed to those in the bulk (surface shifts). The complementary nature of STM and core-level spectroscopy makes the combination of these two techniques an extremely powerful approach, which has been successfully applied to the study of vapor-phase epitaxial growth of Si on Si(100) and Ge(100) using disilane (Si_2H_6) as the source gas.[4,5]

In the present study, we employed the same approach to investigate the growth of Si on Ge(111)-$c(2\times8)$ using disilane. As in previous studies, the growth was performed by first saturating the surface at room temperature with disilane. The hydrogen atoms originating from the disilane molecules were then thermally desorbed, leaving the Si atoms on the surface. The Ge(111)-$c(2\times8)$ surface, however, represents a much more complex reconstruction.[6–8] For either Si(100)-(2×1) or Ge(100)-(2×1), there is only one kind of surface atom; namely, all surface atoms are dimer atoms, each with a dangling bond. In contrast, the Ge(111)-$c(2\times8)$ surface has two kinds of surface atoms with dangling bonds: adatoms and rest atoms. Furthermore, there are two adatoms (rest atoms) in a primitive unit cell, and these two have dissimilar local environments. This complexity in structure makes the study of this system a greater challenge than the (100) systems. Our results show that the initial adsorption configurations of this system are indeed much more complex than the Ge(100) case. Nevertheless, a great deal is learned concerning the processes of disilane adsorption and subsequent thermal decomposition and desorption from the surface. The desorption of hydrogen is found to be accompanied by indiffusion of Si into the Ge substrate. Changes in surface morphology, including formation and coarsening of islands and step flow, are observed.

II. EXPERIMENTAL DETAILS

The photoemission measurements were carried out at the Synchrotron Radiation Center of the University of Wisconsin-Madison. The photocurrent from a gold mesh positioned in the synchrotron beam path was monitored for a relative measure of the incident-photon-beam flux. Photoelectrons were collected and analyzed by a large hemispherical analyzer. The overall energy resolution was better than 0.15 eV. The scanning tunneling microscope used in this study was located in a separate chamber. A tungsten tip was used for acquiring images in a constant current mode.

The Ge(111) samples, of size $0.35\times1.2\times0.04$ cm^3, were sliced from commercial n-type wafers with a resistivity of about 1 Ω cm. After degassing at 700 K for

0163-1829/94/49(3)/1836(8)/$06.00 ©1994 The American Physical Society

many hours, each sample was subjected to cyclic sputtering with a 500-eV Ar^+ ion beam and annealing at ~1100 K for about 30 s to yield a clean and well-ordered surface. Disilane was introduced into the chamber through a precision leak valve. To avoid exciting the disilane molecules, the ionization gauge in the vacuum chamber was turned off during the exposure. The dosing pressure, in the 10^{-5}-torr range, was monitored by the ion-pump current, which was calibrated before the experiment using an ionization gauge. Annealing of the disilane-saturated sample was performed by resistive heating of the sample itself. The temperature of the sample as a function of heating power was calibrated by attaching a very small thermocouple to the center of the front face of an identical test sample.

III. RESULTS AND DISCUSSION

A. STM observation of room-temperature adsorption

The structure of Ge(111)-$c(2\times8)$ is a bulk-terminated surface decorated by $\frac{1}{4}$-monolayer (ML) adatoms located at T_4 sites.[6–8] Figure 1 shows an atomic model in which the two layers of atoms in the top bilayer as well as the adatoms are indicated by circles of difference sizes. Each adatom has a dangling bond and three backbonds attached to three first-layer atoms. The rest of the first-layer atoms not involved in the bonding to the adatoms each have a dangling bond; these are called rest atoms. The rest atoms and the adatoms from the same $c(2\times8)$ pattern related by a spatial offset. A $c(2\times8)$ primitive unit cell is shown in the figure, each containing two adatoms and two rest atoms. The two rest atoms (adatoms) in a unit cell have dissimilar environments. As indicated in the figure, one of the two rest atoms has four nearest-neighbor adatoms forming a rectangle, while the other has three nearest-neighbor adatoms forming a triangle.

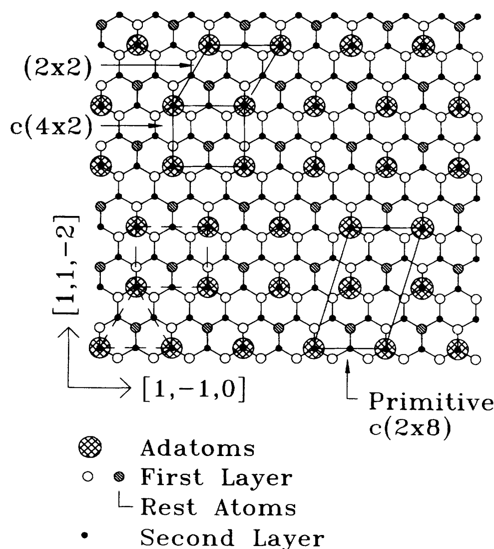

FIG. 1. Atomic model for the Ge(111)-$c(2\times8)$ surface. Each $c(2\times8)$ primitive unit cell consists of a (2×2) unit and a $c(4\times2)$ unit.

There is some electronic charge transfer from the adatoms to the rest atoms,[7] and as a result, STM images taken with a positive (negative) sample bias will mostly show the adatom (rest atom) features on this surface. Each $c(2\times8)$ primitive unit cell can be divided into two units of equal area, one with a local (2×2) symmetry, and the other a local $c(4\times2)$ symmetry, as indicated in the figure. The $c(2\times8)$ pattern is a periodic arrangement of these $c(4\times2)$ and (2×2) units. On typical Ge(111) surfaces, this periodic arrangement of the $c(4\times2)$ and (2×2) units is often disrupted by faults and domain boundaries (due to the threefold symmetry of the surface, there are three possible orientations of the reconstruction).

Figure 2 shows dual-polarity 220×220-Å^2 images of Ge(111)-$c(2\times8)$ exposed to 500 L (1 L=10^{-6} torr s) of disilane at room temperature. The images in Figs. 2(a) and 2(b), acquired simultaneously over the same area with sample bias voltages of -1.5 and $+2.0$ V, respectively, show the spatial distributions of occupied and unoccupied states near the Fermi level.[9] The unoccupied-state image, Fig. 2(b), is dominated by adatom features in the unreacted areas, while the occupied-state image, Fig. 2(a), shows both adatom and rest-atom features. These images also show a domain boundary across the lower-right corner.

Compared to Ge(100)-(2×1) and Si(100)-(2×1), the sticking coefficient of disilane on Ge(111)-$c(2\times8)$ at room temperature is much smaller.[4,5,10,11] The images in Fig. 2 show that even after a 500-L exposure, most of the surface area is still clean. Several kinds of adsorption-induced features can be identified; the main features C, R, S, and T are indicated in Fig. 2(a). Here, S represents a single bright protrusion, T represents three bright protrusions forming a triangle, R represents four bright protrusions forming a rectangle, and C represents larger clusters with unresolved features. In the unoccupied-state image, Fig. 2(b), only the C features can be easily identified.

The R (rectangle) and T (triangle) features in Fig. 2 have been observed before in a study of hydrogen absorption on Ge(111),[12] and we can therefore identify these as due to the adsorption of a single H atom on a Ge rest atom. The triangular and rectangular shapes have to do with the arrangement of neighboring adatoms for the two inequivalent types of rest atoms, as mentioned above. The adsorption of a H atom on a rest atom induces reverse charge transfer making the three or four neighboring adatoms appear more pronounced in occupied-state images. These H atoms on the Ge rest-atom sites must come from the decomposition of the disilane molecules adsorbed on the surface. The presence of GeH radicals on the surface has been confirmed by an infrared study,[13] which shows that disilane adsorption on Ge(111) at room temperature is dissociative and results in a mixture of SiH_3 (minority species), SiH_2, SiH, and GeH radicals on the surface.

We do not know the atomic structures of the S and C features, but they must involve single or multiple adsorption sites of H, SiH, SiH_2, and SiH_3. Each disilane molecule contains two Si atoms; it is most likely that these

two Si atoms will remain close together on the surface after dissociative chemisorption, as is the case for disilane adsorption on Ge(100).[4] Because of the relatively large spatial extent of the *C* feature, our best guess is that it is an adsorption complex involving (at least) two Si atoms and an unknown number of hydrogen atoms. The simplest assignments for the *S* feature is a H atom attached to an adatom dangling bond [a similar feature was observed in hydrogen adsorption on Ge(111), and was attributed to a missing adatom in Ref. 12].

With increasing disilane doses, more reacted areas are observed. Figures 3(a) and 3(b) show dual-voltage images of Ge(111)-$c(2\times8)$ after a 6000-L disilane exposure. The scanned area is 500×500 Å^2. These images have been filtered to remove the low-spatial-frequency components to enhance the local atomic features. Five atomic steps are seen. The reacted regions appear as bright bumps (type-*C* features) in Fig. 3(a). These tend to cluster together. Isolated adsorption features of types *R*, *S*, and *T* can still be found within large $c(2\times8)$ regions, but the areal densities of these features are no larger than those seen in Fig. 2. It appears that the initial adsorption sites act as nuclei for further adsorption in the immediate neighborhood, causing a nonuniform distribution of the

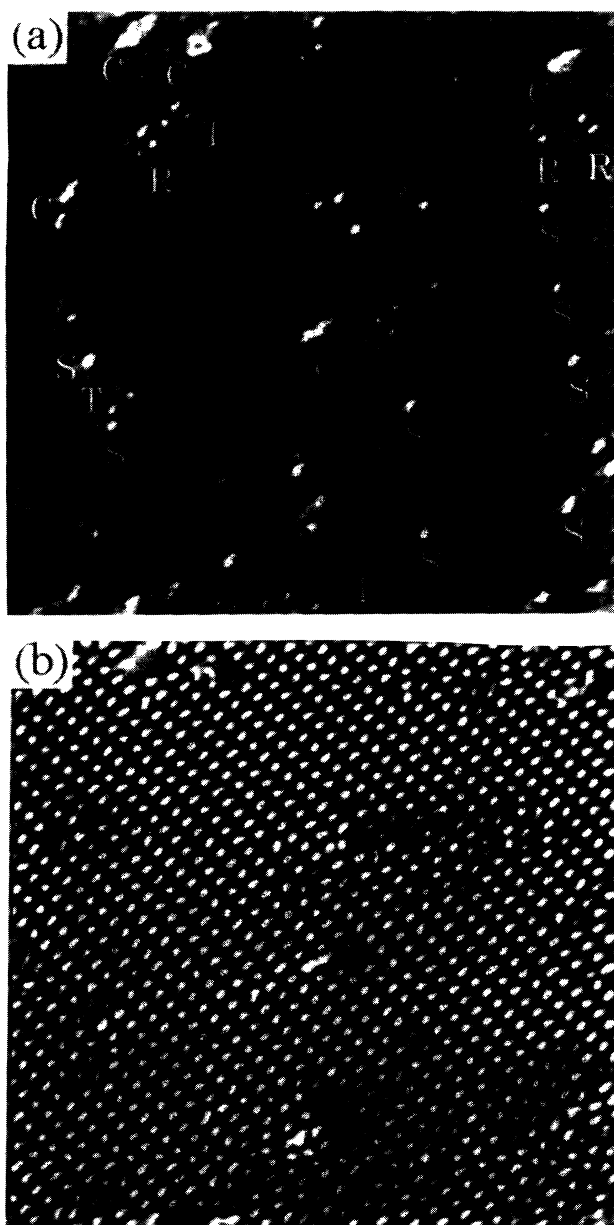

FIG. 2. Dual-voltage STM images for Ge(111)-$c(2\times8)$ after 600-L disilane exposure at 300 K. The scanned area is 220×220 Å^2. The sample bias voltages are (a) -1.5 V and (b) 2.0 V.

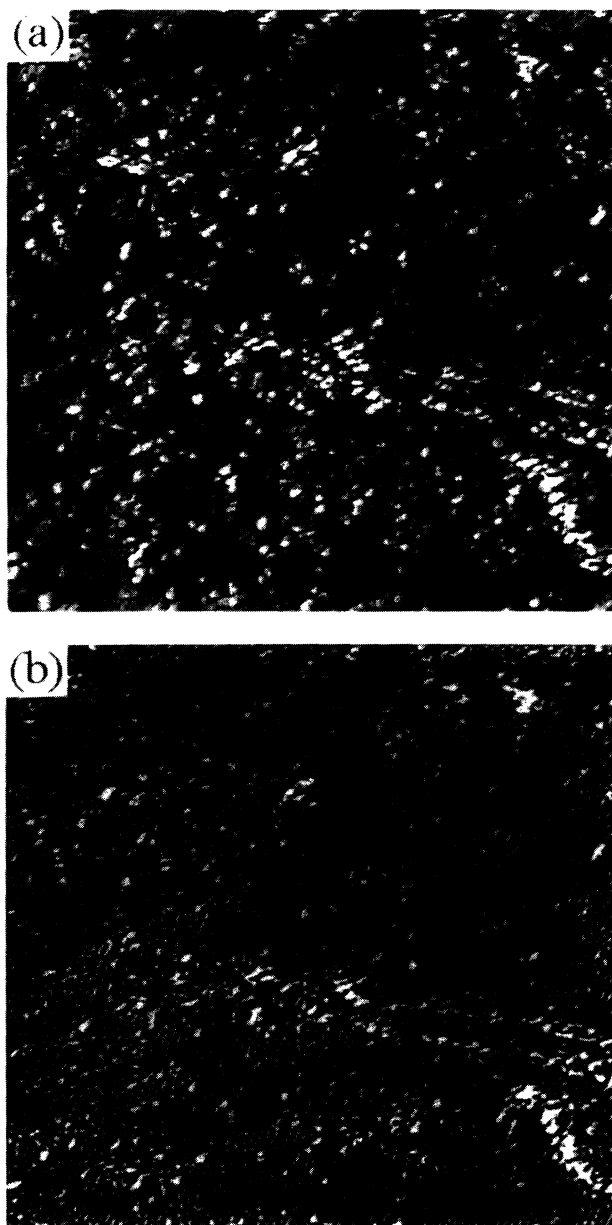

FIG. 3. Dual-voltage STM images for Ge(111)-$c(2\times8)$ after 6000-L disilane exposure at 300 K. The scanned area is 500×500 Å^2. The sample bias voltages are (a) -1.5 V and (b) 2.0 V.

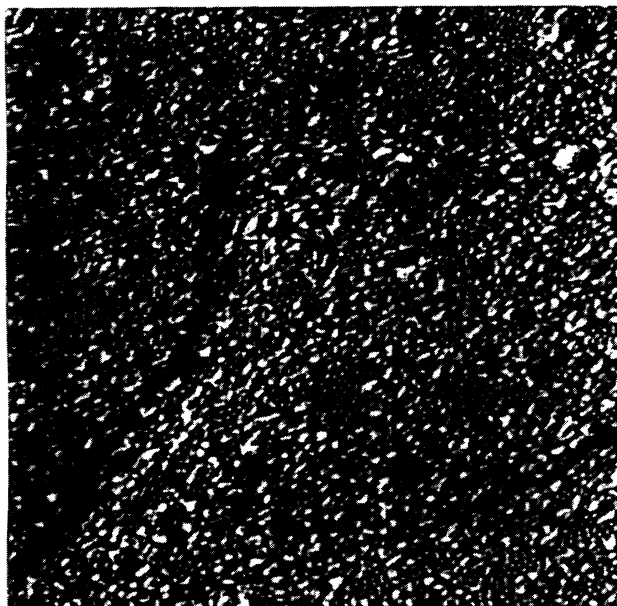

FIG. 4. 500×500 Å^2 STM image for Ge(111)-$c(2\times8)$ after 12 000-L disilane exposure at 300 K. The sample bias voltage is 2.0 V.

reacted areas.

Figures 4 and 5 show unoccupied-state STM images, of size 500×500 Å^2, for 12 000-L and 30 000-L disilane exposures, respectively. In Fig. 4, small areas showing the $c(2\times8)$ adatom pattern are still present. At 30 000-L exposure and beyond, the surface appears to be saturated, as no $c(2\times8)$ regions remain on the surface. The saturated surface is disordered.

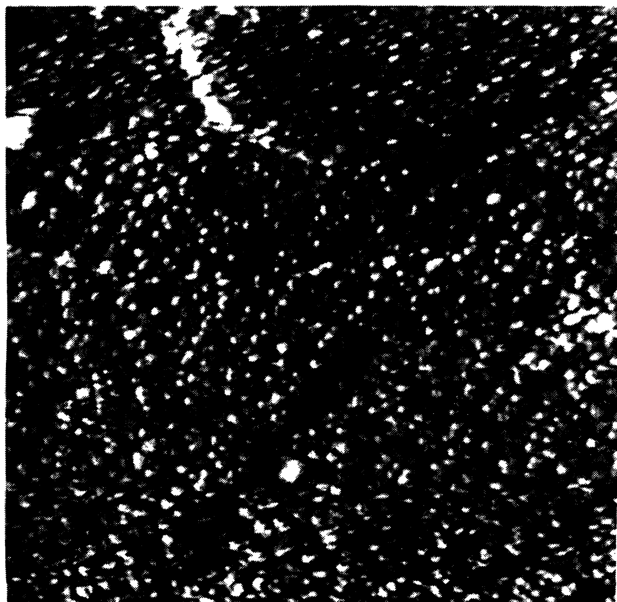

FIG. 5. 500×500 Å^2 STM image for Ge(111)-$c(2\times8)$ after 30 000-L disilane exposure at 300 K. The sample bias voltage is 2.0 V.

B. Si coverage for room-temperature saturated surface

We measured the Si 2p core-level photoemission intensity as a function of disilane exposure. In agreement with the STM observation reported above, the surface becomes saturated at about 30 000-L exposure. To determine the absolute Si coverage for the saturated surface, we compared the Si 2p to Ge 3d intensity ratio for the present system with that of disilane-saturated Ge(100)-(2×1) surface under the same experimental conditions.[4] The saturation Si coverage for the latter system is known to be about $\frac{1}{2}$ (100) atomic layer. Taking into account the different areal atomic densities between the (111) and (100) surfaces, we obtain a Si coverage of about 3.8×10^{14} atoms/cm^2 for the Ge(111) case. This corresponds to about $\frac{1}{2}$ (111) atomic layer.

The reason for our interest here to obtain this coverage is that it is relevant to the process of atomic-layer epitaxy.[14] In this process, the surface is first saturated by adsorption of disilane, and then the hydrogen is desorbed by annealing, leaving the Si on the surface. This quantized deposition can be repeated in a cyclic fashion to build up a film of any desired thickness. For practical applications, it is important to know the net amount of Si deposition in each cycle.

C. Photoemission study of the annealing behavior of the saturated surface

In this part of the experiment, the surface was first saturated by disilane exposure (30 000 L) at room temperature, and then subjected to progressive annealing to higher temperatures. Each anneal lasted 60 s. After each anneal, the sample was allowed to cool down and photoemission spectra were taken. Our interest here is to find out the details of the thermal conversion and desorption processes.

Figure 6 shows Si 2p core-level spectra for various annealing temperatures taken with a photon energy of 140 eV. The relative binding energy scale is referred to the Ge 3$d_{5/2}$ line of the bulk contribution (see below). Using this internal energy reference, we eliminate energy shifts due to changes of surface band bending. The bottom spectrum in Fig. 6 is for the room-temperature saturated surface. The line shape is rather broad, which is expected for a disordered surface. As the annealing temperature increases, the line shape sharpens, as evidenced by the deepening of the valley between the two spin-orbit split peaks. The line shape also shifts toward lower binding energies, and the intensity drops significantly.

The Ge 3d core-level spectra taken with a photon energy of 66 eV for various annealing temperatures are shown in Fig. 7. Also included in this figure is a spectrum obtained from the clean Ge(111)-$c(2\times8)$ surface for comparison. The line shape for the clean surface can be decomposed into three major contributions, B (bulk), $S1$ (surface component one), and $S2$ (surface component two), as shown in previous studies.[15,16] The $S2$ component corresponds to the distinct bump on the low-binding-energy side of the line shape. After the surface is saturated by disilane at room temperature, the line shape

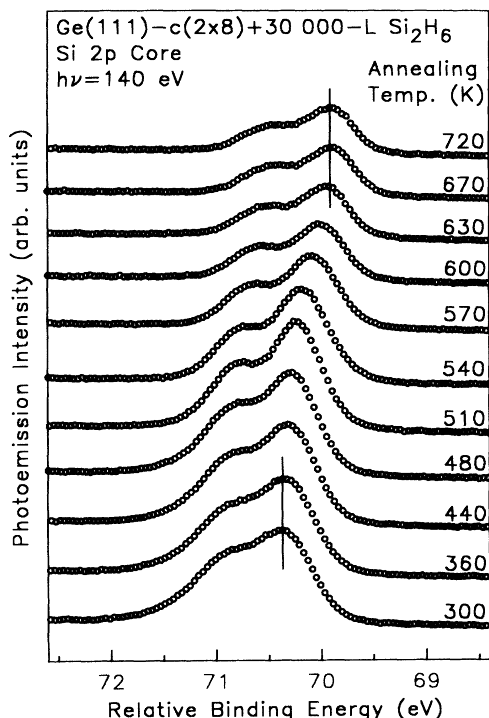

FIG. 6. Photoemission spectra of the Si $2p$ core level for Ge(111) saturated by a 30 000-L disilane exposure at room temperature followed by progressive annealing to various temperatures as indicated. The relative binding energy scale is referred to the Ge $3d_{5/2}$ line of the bulk component. The intensity of each spectrum has been normalized to the incident-photon-beam intensity.

becomes considerably sharper. This is expected since all Ge atoms are now under the surface, and the line shape should become bulklike. As the annealing temperature gets higher, the line shape broadens. This broadening can be attributed to the gradual reappearance of the surface components (see below), and the line shape eventually becomes very similar to that of the clean Ge surface.

The results from a quantitative analysis of the core-level spectra using a least-squares-fitting procedure are summarized in Fig. 8, which shows the integrated Si $2p$ intensity, the binding-energy position of the Si $2p_{3/2}$ peak, and the surface-to-bulk intensity ratios for the two Ge surface components $S1$ and $S2$. Based on these results, we can identify two temperatures $T_1 = 480$ K and $T_2 = 630$ K relevant to the thermal reaction; these are indicated by the vertical dotted lines in the figure. Between these two temperatures, the Si $2p$ intensity drops significantly, while the two Ge surface components gradually reappear.

D. STM observation of the annealing behavior

Figures 9(a)–9(d) show STM images for annealing temperatures of 440, 470, 570, and 650 K, respectively. The sample voltage used was +2.0 V, and the scanned size was 500×500 Å^2. These four annealing temperatures were chosen to be before, at the beginning, in the middle, and after the transition between T_1 and T_2. Comparing Figs. 5, 9(a), and 9(b), it is clear that the surface remains disordered up to T_1; however, there is apparently some coarsening of the cluster structure on the surface as the annealing temperature gets higher. In Fig. 9(c) one sees a number of large islands with poorly defined atomic features. In between these islands, the adatom features on the substrate surface can be seen as bright protrusions. Except for some small patches of $c(2\times8)$, these adatom features show considerable disorder. This disorder is very similar to what has been reported for the growth of Si on Ge(111)-$c(2\times8)$ using molecular-beam epitaxy,[17] and can be described as a breakup of the $c(2\times8)$ pattern into a random arrangement of $c(4\times2)$ and (2×2) units. Figure 9(d) and other pictures that we obtained but not shown here indicate that after the annealing temperature T_2 is reached, the adatom features can be seen for the entire surface. Increasing the annealing temperature causes the islands to coarsen and to be absorbed by step edges (step flow). On large terraces between atomic steps, one can still find some islands separated by denuded zones from neighboring step edges, as seen in Fig. 9(d). The adatom features remain largely disordered due to the fairly random arrangement of the $c(4\times2)$ and (2×2) units.

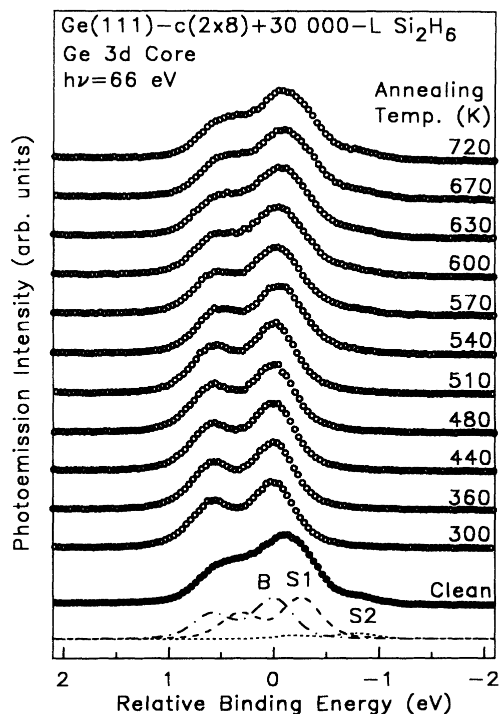

FIG. 7. Photoemission spectra of the Ge $3d$ core level for Ge(111) saturated by a 30 000-L disilane exposure at room temperature followed by progressive annealing to various temperatures as indicated. The relative binding energy scale is referred to the Ge $3d_{5/2}$ line of the bulk component. The intensity of each spectrum has been normalized to the incident-photon-beam intensity. The bottom spectrum is for the clean Ge(111)-$c(2\times8)$ surface, and the decomposition of this spectrum into three components, B, $S1$, and $S2$, are indicated by the curves below.

Again, this disorder is very similar to that for the molecular-beam epitaxial growth of Si on Ge(111)-$c(2\times8)$.

E. Thermal reaction and desorption processes

The above photoemission and STM results together allow a detailed description of the thermal reaction and desorption processes. As mentioned above, the results in Fig. 8 indicate a transition between T_1 and T_2. After the transition, the Ge 3*d* line shape shown in Fig. 7 becomes very similar to that of the starting clean surface. The two surface components reappear, and STM pictures show a complete recovery of the adatom features throughout the entire surface, despite a substantial loss of long-range periodicity of the $c(4\times2)$ and (2×2) units. These results suggest that the resulting surface resembles the clean Ge(111)-$c(2\times8)$ surface. In particular, the reappearance of the two surface components of Ge 3*d* indicates that all hydrogen atoms have desorbed, the surface is now covered by Ge atoms, and the Si atoms must have diffused into the subsurface region. This Si indiffusion is

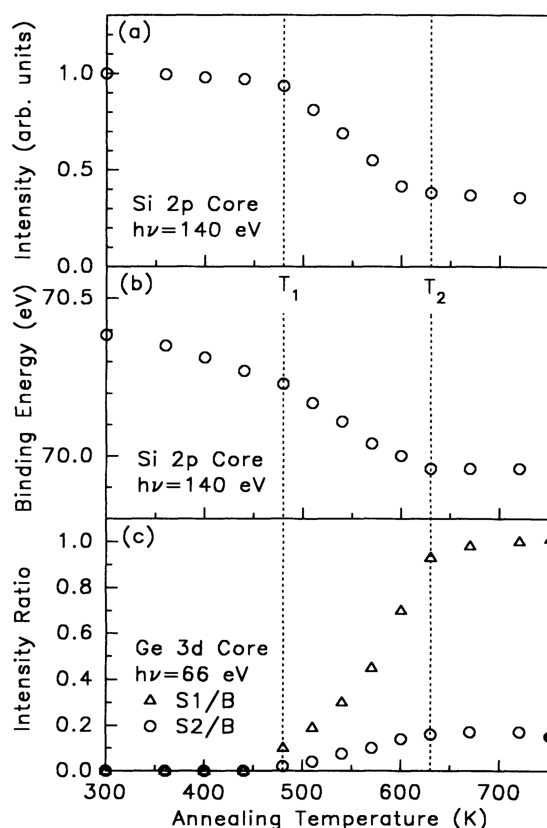

FIG. 8. (a) Integrated intensity of Si 2*p*, (b) binding energy of Si 2*p*, and (c) intensity ratios of the two surface components to the bulk component of Ge, as a function of annealing temperature. The sample is Ge(111)-$c(2\times8)$ initially saturated by a 30 000-L disilane exposure at room temperature. Two temperatures $T_1=480$ K and $T_2=630$ K are indicated by vertical dotted lines. The two data points on the right border of (c), indicated by filled symbols, represent results from the starting clean Ge(111)-$c(2\times8)$ surface.

supported by the data in Fig. 8(a), which shows that the Si 2*p* intensity drops to about 40% of its initial value after annealing to temperatures beyond T_2. The inelastic scattering of the Si 2*p* photoelectrons by the Ge surface layer, governed by a very short electron mean free path,[18] accounts for the intensity reduction. After annealing to beyond T_2, the binding energy of the Si $2p_{3/2}$ core relative to the *B* component of the Ge $3d_{5/2}$ core decreases to 69.96 eV, which is consistent with previous measurements for Si in bulk Ge.[4,19]

The driving force for this Si indiffusion is apparently the lower surface energy of Ge than Si. Similar indiffusion has been observed in the growth of Si on Ge(100) by molecular-beam epitaxy and vapor-phase epitaxy,[4,19] and in the growth of Si on Ge(111) by molecular-beam epitaxy.[17] Although Si and Ge can form an alloy of arbitrary composition, bulk interdiffusion remains negligible for temperatures up to about 900 K.[20] Thus, the indiffusion observed here is a surface effect. As mentioned above, the STM picture shown in Fig. 9(d) resembles those obtained for $\frac{1}{2}$-ML Si on Ge(111)-$c(2\times8)$ deposited by molecular-beam epitaxy.[17] This is not surprising. As soon as all hydrogen atoms are desorbed, the growth kinetics should become the same for these two Si deposition techniques.

The temperature T_1 marks the beginning of the reappearance of the two surface components of Ge, and the beginning of the reduction of the Si 2*p* intensity. Midway between T_1 and T_2, the STM picture in Fig. 9(c) shows that roughly one-half of the surface is covered by islands, which are not well ordered, and these islands are surrounded by areas exhibiting the adatom pattern. This is consistent with the results in Fig. 8 that about one-half of the intensity for each Ge surface component has recovered.

Thermal desorption of H from Ge(111) has been investigated previously by temperature-programmed desorption (TPD) and infrared studies.[13,21] The TPD results show a peak at about 600 K, with significant desorption starting at around 500 K.[21] This is consistent with our measured T_1 of 480 K for the beginning of the recovery of the Ge surface components, and our measured T_2 of 630 K for the completion of the desorption. Desorption of H from pure Si(111) occurs at a much higher temperature.[22] The most likely mechanism for the removal of H from surface Si in the present case is that the H on Si diffuses to neighboring exposed Ge areas from which it desorbs. As soon as the H leaves the Si, the Si atom diffuses into the subsurface region to minimize the surface energy. A similar mechanism has been noted for the thermal reaction of disilane on Ge(100).[4] The indiffused Si atoms remain near the surface, and cause a local perturbation disrupting the long-range order of the $c(4\times2)$ and (2×2) units.

While Figs. 8(a) and 8(c) show no apparent changes between room temperature and T_1, Fig. 8(b) shows a continuous drop of the average Si 2*p* binding energy. This is again similar to the case of disilane on Ge(100), and can be related to the gradual conversion of SiH_3 and SiH_2 radicals on the surface to SiH.[4] During this conversion,

the Si atoms remain on the surface, and so the Si $2p$ intensity and the Ge $3d$ line shape do not change. The reduction of the average Si $2p$ binding energy is related to the reduced chemical shift of Si in going through the sequence from SiH_3, to SiH_2, and to SiH.

F. Comparison with the Ge(100) case

The behavior of the present system is fairly similar to that of disilane growth on Ge(100)-(2×1).[4] For the (100) case, however, the initial adsorption configurations are much simpler, and two separate thermal transitions are observed instead of just one in the present case. As noted above, the room-temperature sticking probability is much lower on the (111) surface. This has a simple explanation. The initial adsorption of a disilane molecule results in two SiH_3 radicals, which will require two dangling bonds on the surface to complete this process. The distance between two neighboring dangling bonds on the (111) surface is much larger than that for the (100) surface, and is much larger than the Si-Si bond length in the disilane molecule. It is likely that this large distance on the (111) surface makes the probability for dissociative chemisorption rather low.

IV. SUMMARY

Core-level photoemission and STM were employed to study the adsorption of disilane on Ge(111)-$c(2\times8)$ at

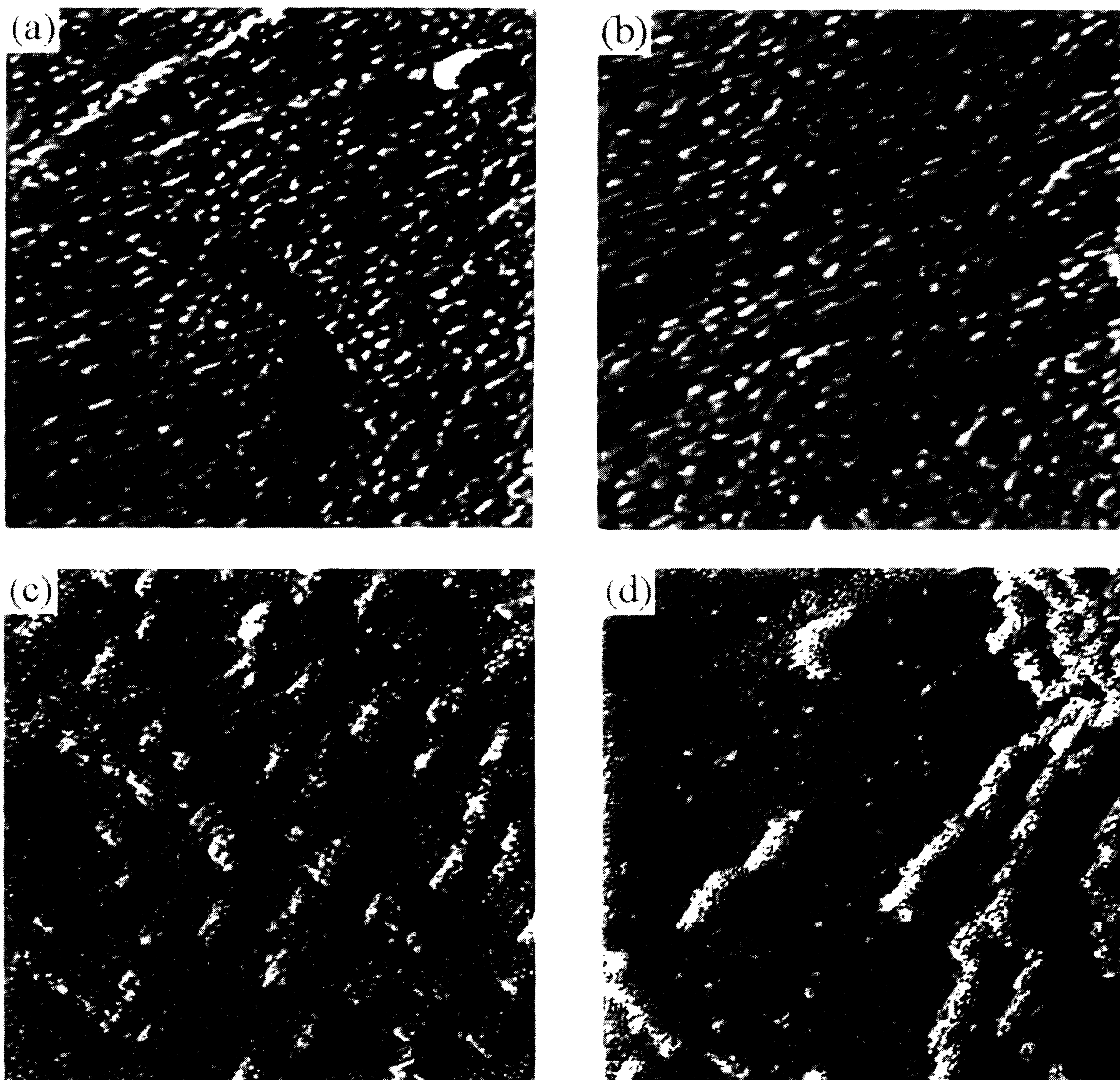

FIG. 9. STM images of Ge(111)-$c(2\times8)$ initially saturated by a 30 000-L disilane exposure after annealing to (a) 440, (b) 470, (c) 570, and (d) 650 K, respectively. The scanned areas are 500×500 Å^2.

room temperature and subsequent decomposition and hydrogen desorption at elevated temperatures. Initial adsorption at room temperature results in the formation of various adsorption configurations on the surface, and identifications and suggestions for the atomic structures are made. The disilane-saturated surface is disordered, with a net Si deposition of about $\frac{1}{2}$ ML. Annealing the saturated surface results in the gradual conversion of SiH_3 to SiH_2 and SiH_2 to SiH. At around 480 K, significant H desorption from GeH commences, and the H on Si begins to also desorb by diffusion from the Si site to neighboring Ge sites. When a SiH radical loses its H, the Si atom moves below the surface, and the Ge surface structure begins to recover. Beyond about 630 K, the desorption of hydrogen is complete, all of the Si atoms have moved below the surface, and the resulting surface shows the spectroscopic characteristics of the clean Ge(111)-$c(2\times8)$ surface. The long-range order associated with the $c(2\times8)$ arrangement of the $c(4\times2)$ and (2×2) units is, however, largely destroyed by the Si atoms which remain in the subsurface region. The STM results for annealing temperatures beyond the temperature for total hydrogen desorption are very similar to the results from molecular-beam epitaxial growth. Island coarsening and step flow are observed.

ACKNOWLEDGMENTS

This material is based upon work supported by the U.S. Department of Energy (Division of Materials Sciences, Office of Basic Energy Sciences), under Grant No. DEFG02-91ER45439. Acknowledgment is also made to the Donors of the Petroleum Research Fund, administered by the American Chemical Society, and to the U.S. National Science Foundation (Grant No. DMR-92-23546) for partial support of the synchrotron beam line operation and personnel. The Synchrotron Radiation Center of the University of Wisconsin at Madison is supported by the National Science Foundation.

[1]S. M. Sze, *Semiconductor Devices, Physics and Technology* (Wiley, New York, 1985).

[2]F. J. Himpsel, F. R. McFeely, J. F. Morar, A. Taleb-Ibrahimi, and J. A. Yarmoff, in *Photoemission and Adsorption Spectroscopy of Solids and Interfaces with Synchrotron Radiation*, Proceedings of the International School of Physics "Enrico Fermi," Course CVIII, Varenna, 1988, edited by G. Scoles (North-Holland, New York, 1991).

[3]T.-C. Chiang, CRC Crit. Rev. Solid State Mater. Sci. **14**, 269 (1988).

[4]D.-S. Lin, T. Miller, and T.-C. Chiang, Phys. Rev. B **47**, 6543 (1993).

[5]D.-S. Lin, T. Miller, T.-C. Chiang, R. Tsu, and J. E. Greene, Phys. Rev. B **48**, 11 846 (1993); D.-S. Lin, E. S. Hirschorn, T.-C. Chiang, R. Tsu, D. Lubben, and J. E. Greene, *ibid.* **45**, 5603 (1992).

[6]R. S. Becker, J. A. Golovochenko, and B. S. Swartzentruber, Phys. Rev. Lett. **54**, 2678 (1985); R. S. Becker, B. S. Swartzentruber, J. S. Vickers, and T. Klitsner, Phys. Rev. B **39**, 1633 (1989).

[7]E. S. Hirschorn, D.-S. Lin, F. M. Leibsle, A. Samsavar, and T.-C. Chiang, Phys. Rev. B **44**, 1403 (1991); Noboru Takeuchi, A. Selloni, and E. Tosatti, Phys. Rev. Lett. **69**, 648 (1992).

[8]J. J. Boland, Science **255**, 186 (1992).

[9]R. M. Tromp, R. J. Hamers, and J. E. Demuth, Science **234**, 304 (1986).

[10]J. J. Boland, Phys. Rev. B **44**, 1383 (1991).

[11]J. Wintterlin and Ph. Avouris, Surf. Sci. Lett. **286**, 523 (1993).

[12]T. Klitsner and J. S. Nelson, Phys. Rev. Lett. **67**, 3800 (1991).

[13]J. E. Crowell and G. Lu, J. Electron Spectrosc. Relat. Phenom. **54/55**, 1045 (1990).

[14]D. Lubben, R. Tsu, T. R. Bramblett, and J. E. Greene, J. Vac. Sci. Technol. A **9**, 3003 (1991); H. Hirayama, T. Tatsumi, and N. Aizaki, Appl. Phys. Lett. **52**, 1484 (1988).

[15]K. Hricovini, G. Le Lay, M. Abraham, and J. E. Bonnet, Phys. Rev. B **41**, 1258 (1990); R. D. Schnell, F. J. Himpsel, A. Bogen, D. Rieger, and W. Steinmann, *ibid.* **32**, 8052 (1985).

[16]J. A. Carlisle, T. Miller, and T.-C. Chiang, Phys. Rev. B **45**, 3811 (1992).

[17]D.-S. Lin, H. Hong, T. Miller, and T.-C. Chiang (unpublished).

[18]F. J. Himpsel, P. Heimann, T.-C. Chiang, and D. E. Eastman, Phys. Rev. Lett. **45**, 1112 (1980).

[19]D.-S. Lin, T. Miller, and T.-C. Chiang, Phys. Rev. B **45**, 11 415 (1992).

[20]A. J. Hoeven, J. Aarts, and P. K. Larsen, J. Vac. Sci. Technol. A **7**, 5 (1989).

[21]L. Surnev and M. Tikhov, Surf. Sci. **138**, 40 (1984).

[22]J. A. Schaefer, J. Q. Broughton, J. C. Bean, and H. H. Farrell, Phys. Rev. B **33**, 2999 (1986); H. H. Farrell, J. Q. Broughton, J. A. Schaefer, and J. C. Bean, J. Vac. Sci. Technol. A **4**, 123 (1986).

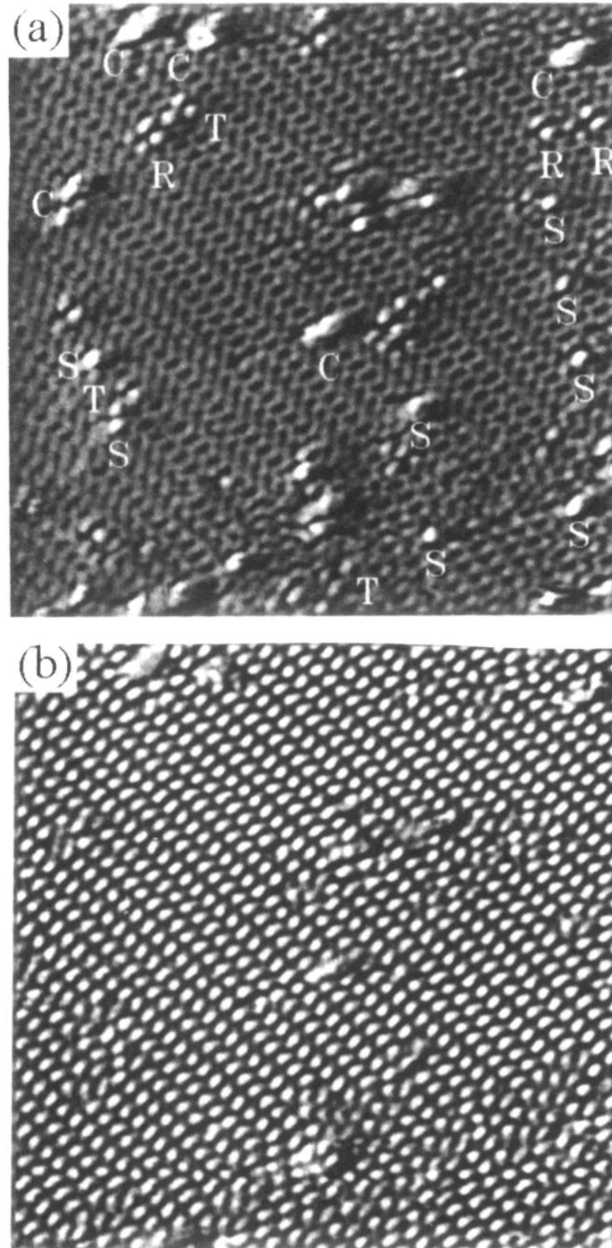

FIG. 2. Dual-voltage STM images for Ge(111)-$c(2\times8)$ after 600-L disilane exposure at 300 K. The scanned area is 220×220 $\mathrm{\AA}^2$. The sample bias voltages are (a) -1.5 V and (b) 2.0 V.

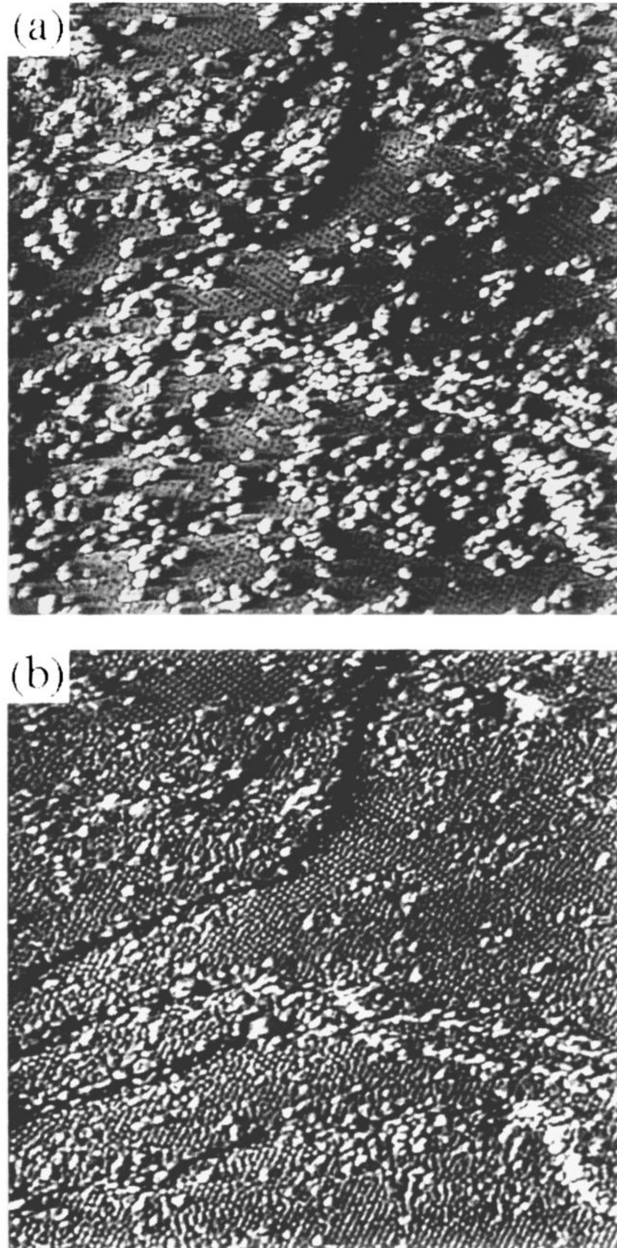

FIG. 3. Dual-voltage STM images for Ge(111)-$c(2\times8)$ after 6000-L disilane exposure at 300 K. The scanned area is 500×500 Å^2. The sample bias voltages are (a) -1.5 V and (b) 2.0 V.

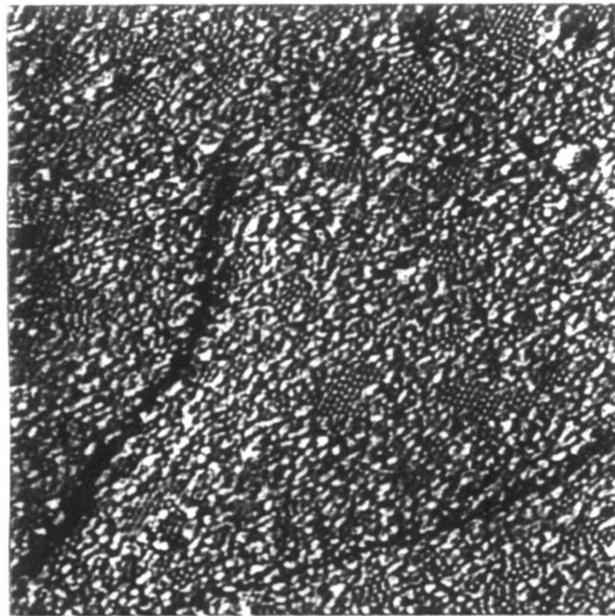

FIG. 4. 500×500 Å^2 STM image for Ge(111)-$c(2\times8)$ after 12 000-L disilane exposure at 300 K. The sample bias voltage is 2.0 V.

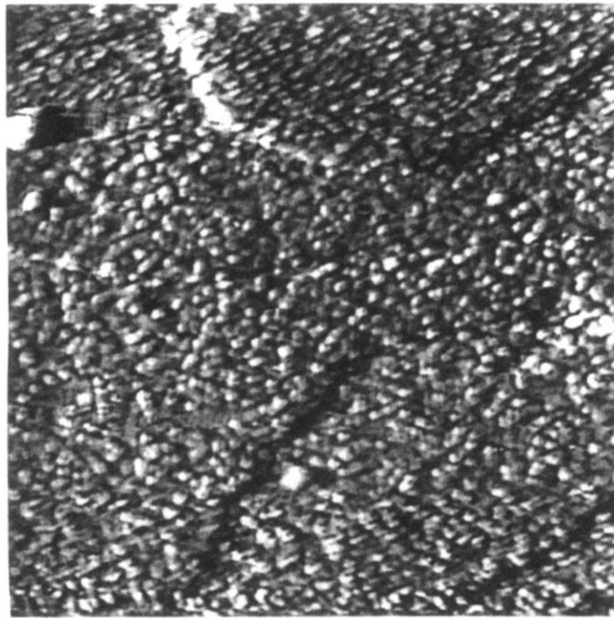

FIG. 5. 500×500 Å^2 STM image for Ge(111)-$c(2\times8)$ after 30 000-L disilane exposure at 300 K. The sample bias voltage is 2.0 V.

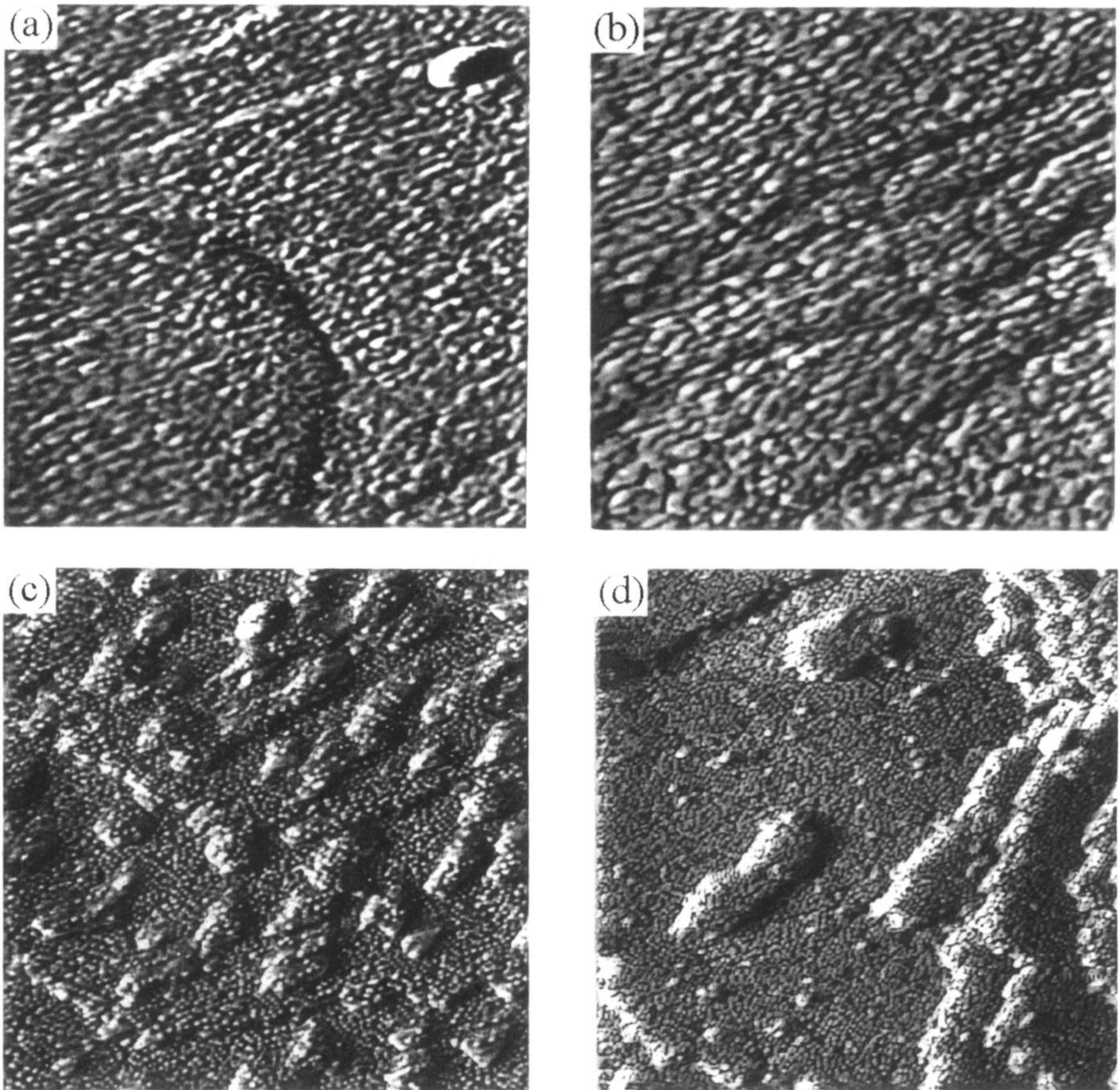

FIG. 9. STM images of Ge(111)-$c(2\times8)$ initially saturated by a 30 000-L disilane exposure after annealing to (a) 440, (b) 470, (c) 570, and (d) 650 K, respectively. The scanned areas are 500×500 Å^2.